

The BCC unit cell for latticed SLM parts; mechanical properties as a function of cell size.

I. Maskery,¹ A.O. Aremu,¹ M. Simonelli,¹ C. Tuck,¹
R.D. Wildman,¹ I.A. Ashcroft,¹ and R.J.M. Hague¹

¹*Faculty of Engineering, University of Nottingham, Nottingham NG7 2RD, UK*

REVIEWED

The existing framework describing the mechanical properties of lattices places strong emphasis on one important property, the relative density of the repeating cells. In this work, we explore the effects of cell size, attempting to construct more complete models for the performance of lattices. This was achieved by examining the elastic modulus and ultimate tensile strength of latticed parts with a range of unit cell sizes and fixed density. The parts were produced by selective laser melting (SLM). The examined cell type was body-centred-cubic (BCC), a cell of high relevance for SLM because of its self-supporting structure. We obtained power law relationships for the mechanical properties of our latticed specimens as a function of cell size, which are similar in form to the existing laws for the density dependence. These can be used to predict the properties of latticed column structures comprised of BCC cells, and may be easily amended for other situations. In addition, we propose a novel way to analyse the elastic modulus data, which may lead to more general models, applicable to parts of varying size. Lastly, our general methodology may be of use in future studies which explore the other parameters that determine lattice performance; the choice of cell type, the global shape of the lattice structure and the type of stress.

Keywords: selective laser melting; lattice; aluminium alloy

INTRODUCTION

One of the most promising capabilities of additive manufacturing (AM) is the production of novel lightweight structures which, of course, are in high demand across sectors such as automotive, medicine and aerospace. Many innovations in this field have come from the use of topology optimisation as a design tool, which is typically used to identify the material layout that maximises specific mechanical properties[1–3].

An alternate and complementary route to better parts, one that is enabled by the manufacturing freedoms of AM, is the replacement of otherwise solid volumes with lattice structures. Such designs have the potential to deliver large reductions in part weight, while also offering high levels of energy absorption under static and dynamic loading[4–8]. However, the choice of lattice unit cell design is large and the mechanical properties of different cell types are far from fully understood. This is a major obstacle in the development of design methods that utilise lattice structures effectively.

Beside the choice of cell type (body-centred-cubic (BCC), face-centred-cubic (FCC), gyroidal, hexahedral, to provide a few examples), at least two other cell properties are significant in determining its mechanical performance; its relative density (also known as its volume fraction) and its size. The first of these factors has received some prior attention, largely because of the similarity between lattice structures and the more well established foams, while the second has received virtually none.

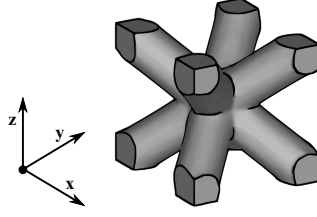


FIG. 1: The BCC unit cell with a relative density, ρ^* , of 0.36.

This work examines the elastic modulus and ultimate tensile strength of latticed parts with BCC unit cells of varying size and fixed density. The parts were produced in Ti-6Al-4V alloy using selective laser melting (SLM) and the cell type was chosen because it is known to be self-supporting (it includes no horizontal members) and has been examined experimentally and theoretically elsewhere[5, 6, 9, 10]. The main aim of the investigation is to uncover how the mechanical properties of lattice structures vary according to size of the chosen unit cell. We will attempt to explain the origins of these relationships and add our findings to the semi-empirical models that currently exist.

The Gibson-Ashby model

Gibson and Ashby analysed the mechanical properties of metal and polymer foams by considering them as systems of open or closed regular cells, expanding upon other work on honeycomb structures[11, 12]. They used analytical methods based on the beam theory of Timoshenko and Goodier[13], and Roark and Young[14] to relate several properties (the elastic modulus and plastic yield strength, amongst others) of a foam under compression or tension to its relative density, ρ^* . The relationships put forward by Gibson and Ashby were seen to describe the mechanical behaviour of several foams adequately[11, 15, 16]. The equations have since been applied to latticed structures comprising repeating regular unit cells, an application they were essentially devised for[4, 17, 18].

Before presenting Ashby and Gibson's relationships, some properties of a lattice structure must be defined. We have that,

$$\rho^* = \rho_{\text{latt.}} / \rho_{\text{sol.}}, \quad (1)$$

where $\rho_{\text{latt.}}$ and $\rho_{\text{sol.}}$ are the densities of a lattice structure and a fully-dense solid, respectively (both composed of the same material). In this way, ρ^* , can be seen simply as the fraction of a particular volume taken up by the solid material of the lattice. Similarly, we can define,

$$E^* = E_{\text{latt.}} / E_{\text{sol.}}, \quad (2a)$$

$$\sigma_U^* = \sigma_{U \text{ latt.}} / \sigma_{U \text{ sol.}}, \quad (2b)$$

so that E^* and σ_U^* are the elastic modulus and ultimate tensile strength of a lattice represented as fractions of those of a fully-dense solid of the same material. These will henceforth be referred to as the relative elastic modulus and relative ultimate tensile

strength.

Gibson and Ashby laid down the straightforward scaling relationship for E^* as a function of the relative density[11, 12, 19];

$$E^* = C_1 \rho^{*m}, \quad (3)$$

where the exponent m varies depending on the relative contributions of stretching and bending in the cellular deformation process; it is given as $m = 2$ for open, bending-dominated, cell types, with additional terms being added to equation 3 to account for membrane stresses and gas pressure effects in closed cells. The prefactor C_1 , “includes all of the geometric constants of proportionality[11],” and therefore varies significantly according to the specimens being examined.

The issue of ultimate tensile strength is a little more involved, with a simple relationship of the form of equation 3 not forthcoming. Instead, for an open-celled lattice under compression, Gibson and Ashby provided,

$$\sigma_{cr}^* \propto l_c^{(-\frac{3}{m_w})} \rho^{*(\frac{3}{2}-\frac{1}{m_w})}, \quad (4)$$

for the crushing strength, σ_{cr}^* , as a function of cell width, l_c , and relative density. m_w is the Weibull modulus, a parameter used to quantify the variance in strength amongst samples of brittle parts. It is related to the distribution of flaws in the material and, in this case, it principally dictates the size dependence of the part strength; the larger the Weibull modulus, the smaller the reduction in strength due to increasing part size. Physically, this is due to the fact that larger parts are more likely to contain larger pre-existing cracks or pores.

For an open-celled lattice under tension, Gibson and Ashby similarly provided,

$$K_{IC}^* \propto l_c^{(\frac{1}{2}-\frac{3}{m_w})} \rho^{*(\frac{3}{2}-\frac{1}{m_w})}, \quad (5)$$

to describe the fracture toughness, K_{IC}^* , again, as a function of cell width and relative density. In this case, $m_w = 6$ is a limit; the fracture toughness increases with cell size if $m_w > 6$ and decreases with cell size if $m_w < 6$.

The cell size dependence for the mechanical properties

Part of the motivation for this work stems from the recognition that Gibson and Ashby’s parameter C_1 , introduced in equation 3, must subsume virtually all of the geometrical information about the lattice except for its relative density. The factors which are thought to determine this parameter are; (i) the choice of unit cell type, of which there are a great many with different potential applications and varying suitability for SLM (and AM in general), (ii) the global shape of the lattice structure, (iii) the type of stress, and (iv) the size of the repeating unit cell. This work focuses on the last of these properties, posing the question: with fixed relative density, how does the unit cell size affect the elastic modulus of a lattice? Information in response to this question could be used to develop more effective methods for predicting the moduli of latticed parts, and would therefore be highly valuable as a design tool.

	Gauge width (mm)	
	5.00	7.00
Unit cell width (mm)	1.00	1.00
	1.66	-
	2.50	3.50
	5.00	7.00

TABLE I: The range of unit cell widths for the two types of test specimen.

With respect to the relative ultimate tensile strength of the lattices, a cell size dependence is essentially predicted, though the form it takes has not been explicitly laid out. We will attempt to identify this dependence and relate it to the existing theory for the closely related properties from equations 4 and 5. Once again, any knowledge gleaned regarding the performance of lattices with different sized cells, and equivalent density, could be useful in the development of methods to design lattices to meet specific load conditions.

EXPERIMENTAL DETAILS

Specimen production

Tensile test specimens with square cross-section were designed according to the ISO standard 6892-1:2009. Specimens with two gauge widths, 5 and 7 mm, were examined. The gauge volumes comprised a repeating BCC unit cell of varying size contained within a ‘net skin’ (determined after production to have thickness 0.243 ± 0.007 mm). The net skin was employed so that an extensometer could be fitted to the exterior of the gauge surfaces, allowing accurate strain measurements. The BCC unit cell, which in our work had a relative density of 0.36, is illustrated in figure 1.

The specimen details, that is, the range of unit cell sizes for each tensile bar, are provided in table I. Figures 2 and 3 are CAD representations of the tensile specimens; the former shows both the 5 and 7 mm gauge versions of the part, including dimensions, while the latter provides a comparison of a latticed gauge region with and without the net skin, revealing the BCC cells beneath. Several parts with solid gauge volumes were also examined, so that the relative mechanical performance of the latticed specimens could be determined.

The specimens were provided by Renishaw Plc. They were manufactured from Ti-6Al-4V using a Renishaw AM250 SLM machine. The laser power, laser scan speed and hatch spacing were 200 W, 600 mm/s and 150 μ m, respectively, and a ‘meander’ scanning strategy was taken, whereby the hatch path of each subsequent layer was rotated by 67° from the previous one. This strategy serves to reduce any anisotropy, geometric or mechanical, that might occur if there were no hatch rotation. The test specimens underwent a stress relieving heat treatment (600 $^\circ$ C for 3 hours under an Ar-rich atmosphere) before removal

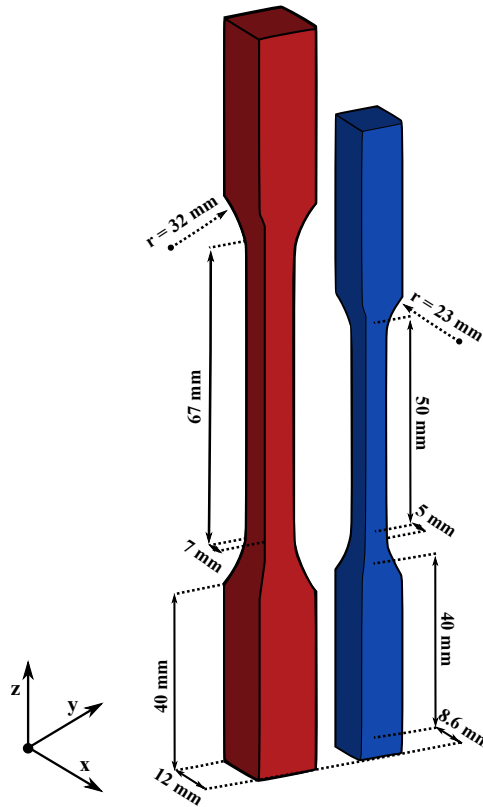


FIG. 2: CAD drawings of the 5 mm gauge (right) and 7 mm gauge (left) tensile specimens, including dimensions.

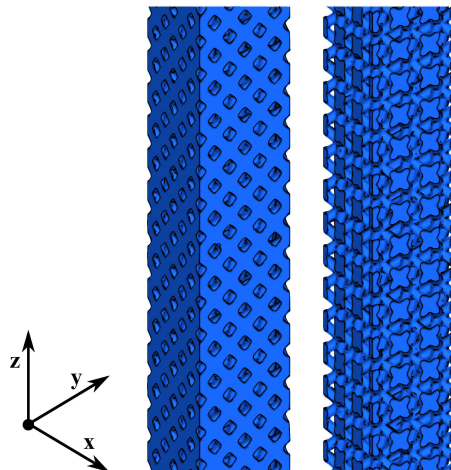


FIG. 3: CAD drawing of the latticed region of the 5 mm gauge specimen with 1.66 mm unit cells. The region is shown with (left) and without (right) the net skin that was employed so that a surface-mounted extensometer could be used during testing.

from the build plate. Figure 4 shows a selection of the 7 mm gauge width specimens prior to testing, including one which is fully solid and two latticed parts with unit cells of width 3.50 and 7.00 mm.

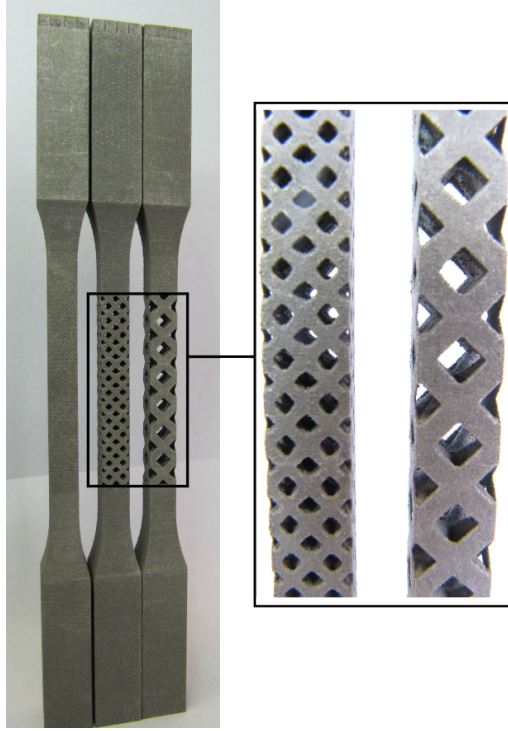


FIG. 4: Photographs of a selection of 7 mm gauge parts. From left to right; solid gauge section, 3.50 mm unit cell and 7.00 mm unit cell. The inset shows a close-up of the latticed regions, with the net skin and internal spars visible.

Tensile testing

Elastic moduli, $E_{\text{latt.}}$, and ultimate tensile strengths, $\sigma_{U \text{ latt.}}$, were recorded for the latticed 5 and 7 mm test bars. All measurements were made using an Instron-5969 universal testing machine. The tensile strain was applied at a rate of 0.01 mm/s. An Instron series 2630 extensometer with 25 mm gauge length was clamped to the center of the latticed section of each test specimen in order to record the strain. Elastic moduli were determined from the regions up to 0.5% strain of the experimental stress-strain curves. Measurements were performed on at least two, and usually three, specimens per design (each combination of cell size and gauge width), with the means and standard errors being used for subsequent analysis.

The moduli of completely solid (non-latticed) test specimens were also recorded. These were 102.3 ± 0.9 and 101 ± 1 GPa for the 5 and 7 mm bars, respectively, and provide the $E_{\text{sol.}}$ of equation 2a. They agree with each other within experimental error and are slightly lower than values typically associated with cast and forged alloys ($\sim 105 - 116$ GPa[20, 21]). The ultimate tensile strength of the solid bars was found to be 1.07 ± 0.01 GPa, slightly higher than expected from cast alloy but lower than has been reported for some Ti-6Al-4V SLM parts[21–23]. This value constitutes $\sigma_{U \text{ sol.}}$ of equation 2b.

RESULTS AND DISCUSSION

Numerical results from the mechanical testing of all specimens are provided in table II, where the relative properties, E^* and σ_U^* , are as defined in equations 2a and 2b. The

	l_c (mm)	v_c (mm ³)	v^* $\times 10^{-3}$	$E_{\text{latt.}}$ (GPa)	E^* $\times 10^{-3}$	σ_U latt. (MPa)	σ_U^* $\times 10^{-3}$
5 mm gauge bars	1.00	1.00	1.10	17.2 ± 0.5	169 ± 6	189 ± 1	177 ± 2
	1.66	4.63	5.30	12.0 ± 0.5	118 ± 5	152 ± 1	141 ± 2
	2.50	15.6	17.9	10.2 ± 0.3	100 ± 3	117.3 ± 0.4	109 ± 1
	5.00	125	143	7.8 ± 0.3	76 ± 3	68.8 ± 0.8	64 ± 1
7 mm gauge bars	1.00	1.00	0.42	19.7 ± 0.4	194 ± 5	174 ± 4	163 ± 4
	3.50	42.9	17.9	9.0 ± 0.3	89 ± 1	102 ± 1	95 ± 1
	7.00	343	143	7.0 ± 0.5	70 ± 5	55 ± 2	52 ± 2

TABLE II: Absolute and relative mechanical properties of the latticed specimens for varying unit cell sizes. The relative properties (v^* , E^* , and σ_U^*) are defined in the text.

unit cell volumes, v_c , for each specimen type are also included; for BCC cells these are simply the unit cell width cubed. v^* is a property which will be defined and discussed shortly.

The elastic modulus

The relative elastic moduli are plotted in figure 5 as a function of cell width. The E^* values decrease over the examined range of cell width, from $(19.4 \pm 0.5)\%$ to $(7.0 \pm 0.5)\%$ of the $E_{\text{sol.}}$ values obtained from solid bars. The second feature of note is that the data from both the 5 and 7 mm test bars follow the same distribution, signifying that we may treat them as a single data set for the purposes of data analysis.

We first hypothesize that E^* follows a power law with l_c similar to that already known to exist for ρ^* . We suggest,

$$E^* = U_1 l_c^{n_1}, \quad (6)$$

where U_1 and n_1 are analogous to Gibson and Ashby's C_1 and m of equation 3. The resulting weighted least-squares fit is shown as a dashed line in figure 5. The values of U_1 and n_1 were found to be 0.179 ± 0.009 and -0.56 ± 0.05 , respectively. However, this fit is statistically rather poor, with a $\bar{\chi}^2$ (reduced- χ^2) value of 2.29, and the fit residual, shown in the upper panel of figure 6, shows significant additional structure. Clearly, this simple model is incapable of describing the data set well.

Two variations on this scaling law were also trialled; one with a constant to modify the cell width, the other with a constant to modify the relative elastic modulus. Physically, such constants could be interpreted as systematic errors associated with the experimental procedure, or they might be true requirements of the model required to describe the data. The modified power laws are given by $E^* = U_1 (l_c + \delta_{l_c})^{n_1}$ and $E^* = U_1 l_c^{n_1} + \delta_{E^*}$, and are shown in figure 5 as solid and dotted lines, respectively. As anticipated, the $\bar{\chi}^2$ values associated with these fits are much improved, with the former providing a value very close to unity. Furthermore, the central panel of figure 6 shows far less residual structure for

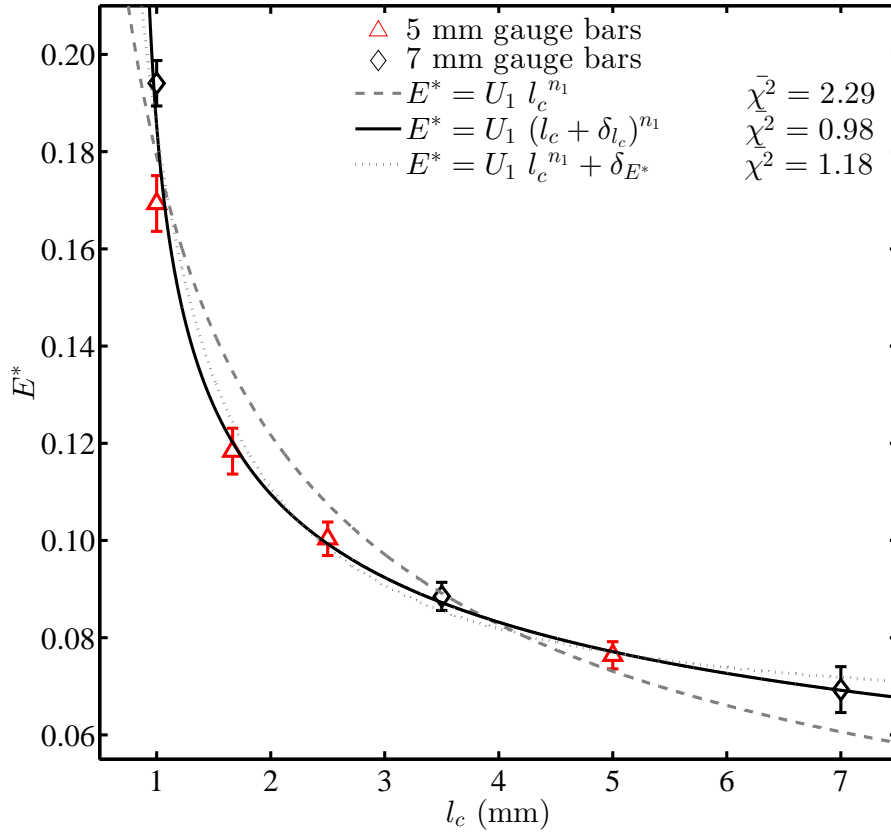


FIG. 5: The relative elastic modulus, E^* , of the 5 and 7 mm latticed test bars as a function of cell width, l_c . Weighted least-squares power law fits are shown as dashed, solid and dotted lines. The fitting procedure is described in the text.

the $E^* = U_1 (l_c + \delta_{l_c})^{n_1}$ fit, compared to the the unmodified form. The parameters from this fit were $U_1 = 0.11 \pm 0.01$, $\delta_{l_c} = -0.8 \pm 0.1$ mm and $n_1 = -0.28 \pm 0.07$. The determined cell width offset of -0.8 mm could be indicative of a systematic error in the manufacture of the latticed bars. However, this issue was subsequently investigated; the cell widths were found to conform well to the expected values.

The second modified power law, $E^* = U_1 l_c^{n_1} + \delta_{E^*}$, provides a poorer fit than that described above, with $\chi^2 = 1.18$ and more residual structure, but it is still superior to the unmodified form. The fitted parameters are $U_1 = 0.12 \pm 0.01$, $n_1 = -1.3 \pm 0.4$ and $\delta_{E^*} = 0.06 \pm 0.01$.

Anomalous behaviour of the smallest cells

Furthering the analysis of the $E^*(l_c)$ data, we speculate that data from 1 mm cells in both the 5 and 7 mm latticed test bars may be outliers or simply not described by the same mathematical model that describes the rest of the data set. Evidence for this assertion comes from the residuals in figure 6, where the 1 mm data are almost equally poorly described by all three models trialled so far. There may be a physical cause for this; the cavities, or voids, in the 1 mm lattice structures are small enough for the complete removal of Ti-6Al-4V powder to be problematic. If residual powder remained

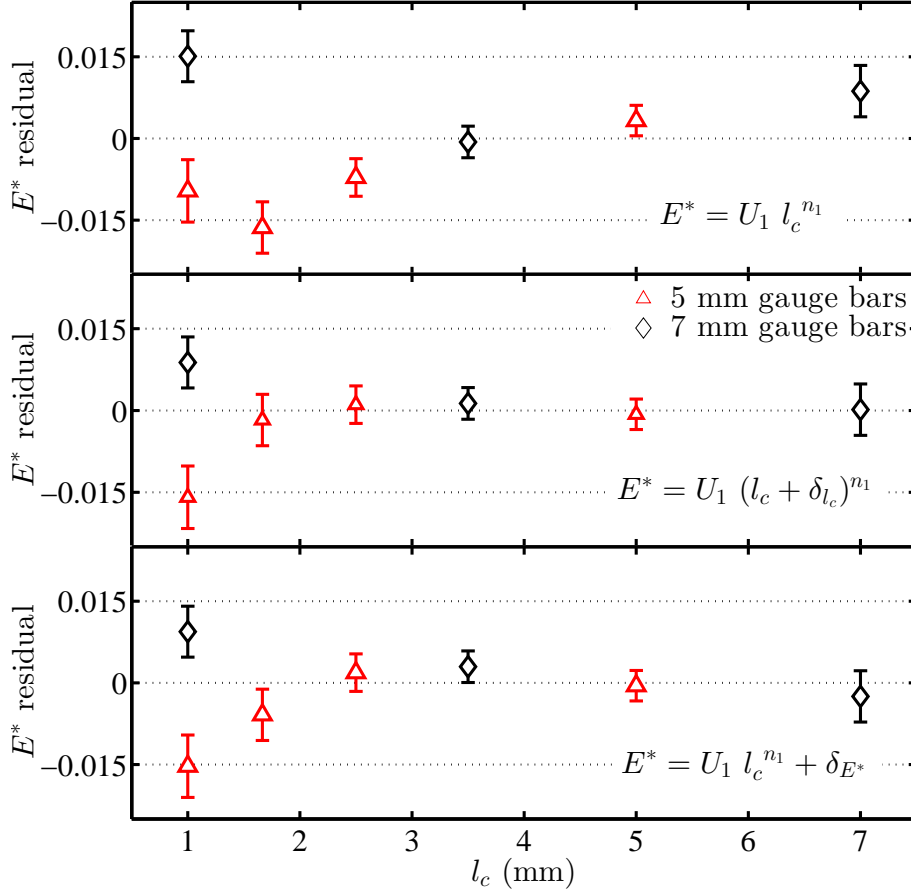


FIG. 6: Residuals from the relative elastic modulus fits of figure 5.

in some or many of the internal lattice cavities for the 1 mm cells, the behaviour of those bars under tension may be quite different from the others. Another possible explanation is that the performance of these cells is being affected by the presence of loosely bound powder around the lattice struts and nodes. Loosely bound, or partially sintered, powder is a persistent issue in SLM and affects different materials to different extents, often negatively impacting properties such as the surface roughness; its presence is related to the choice of laser processing parameters and the morphology of the powder. In the case of our latticed structures, it would have a larger effect for smaller cells, where the dimensions of the struts and nodes are smallest.

The relative elastic moduli were re-fit with $E^* = U_1 l_c^{n_1}$, this time excluding those data from the 1 mm cells; the result is shown in figure 7. The parameters are $U_1 = 0.144 \pm 0.002$ and $n_2 = -0.130 \pm 0.004$. The $\bar{\chi}^2$ value is extremely low at 0.02, most likely indicating that, with the exclusion of two data points (and the reduction to just three degrees of freedom for the fitting procedure), the fit is over-paramaterised.

Alternate analysis

In figure 8 we present E^* as a function of the *relative* cell volume, v^* . This, we define as,

$$v^* = v_c / v_{\text{latt. env.}}, \quad (7)$$

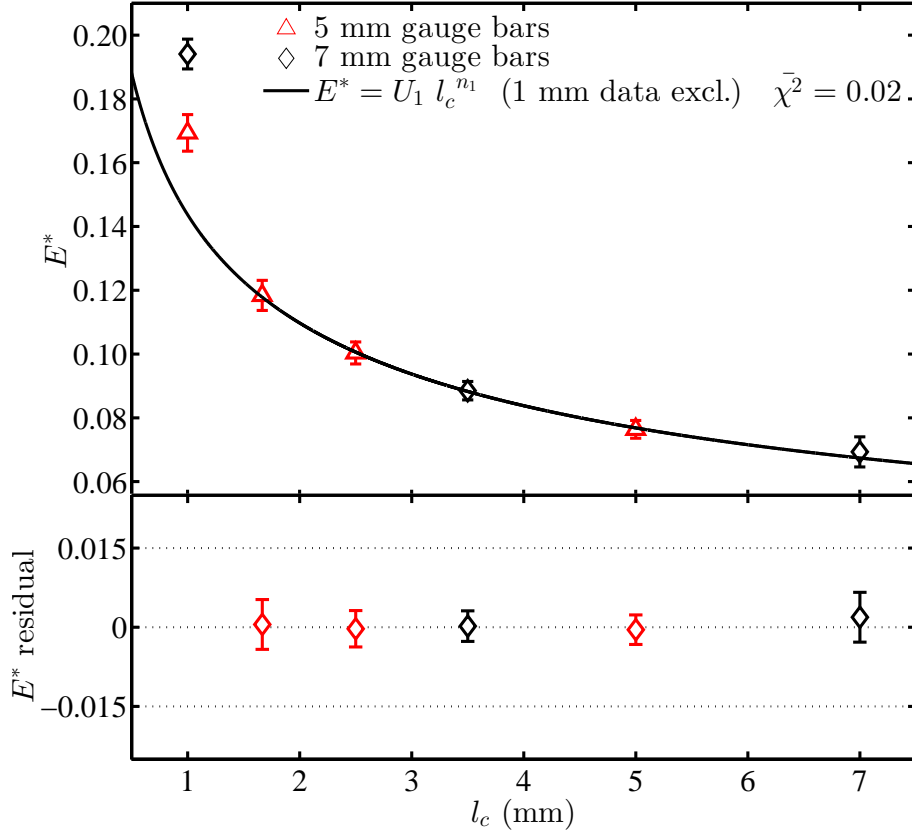


FIG. 7: 5 and 7 mm E^* data fit with $E^* = U_1 l_c^{n_1}$. Data from the 1 mm cells are excluded from the fit, as described in the text. The lower panel shows the corresponding fit residual.

where v_c is the cell volume (given simply by l_c^3) and $v_{\text{latt. env.}}$ is the volume of the latticed environment in which the cell resides. For the 5 and 7 mm bars, $v_{\text{latt. env.}}$ has values 875 and 2401 mm³, respectively (i.e. $5 \times 5 \times 35$ mm and $7 \times 7 \times 49$ mm, where 35 and 49 mm are the lengths of the latticed gauge sections of the bars).

Choosing to work with a relative measure of cell size like v^* , rather than the absolute values of l_c or v_c , may provide a way to formulate general descriptions of lattices that are independent of the size of the part, equally applicable to parts of quite different length scales. There is precedent for this methodology in the way we work with E^* , for example, instead of E . This is done so that general rules, such as equations 3, 4 and 5, may be developed that apply to a range of materials, including polymers, ceramics and metals, where the absolute moduli differ greatly. Similarly, ρ^* is used instead of ρ because the absolute densities of the materials in question also vary significantly.

An unmodified power law was applied and it is shown as a solid line in figure 8. Weighted least-squares fitting provided the result; $E^* = (0.051 \pm 0.004) v^{*(-0.17 \pm 0.01)}$ with $\bar{\chi}^2 = 1.68$. The fit is statistically poorer than the previous best, but it has the advantage of describing the E^* behaviour equally well over the full range of cell size, including the smallest cells.

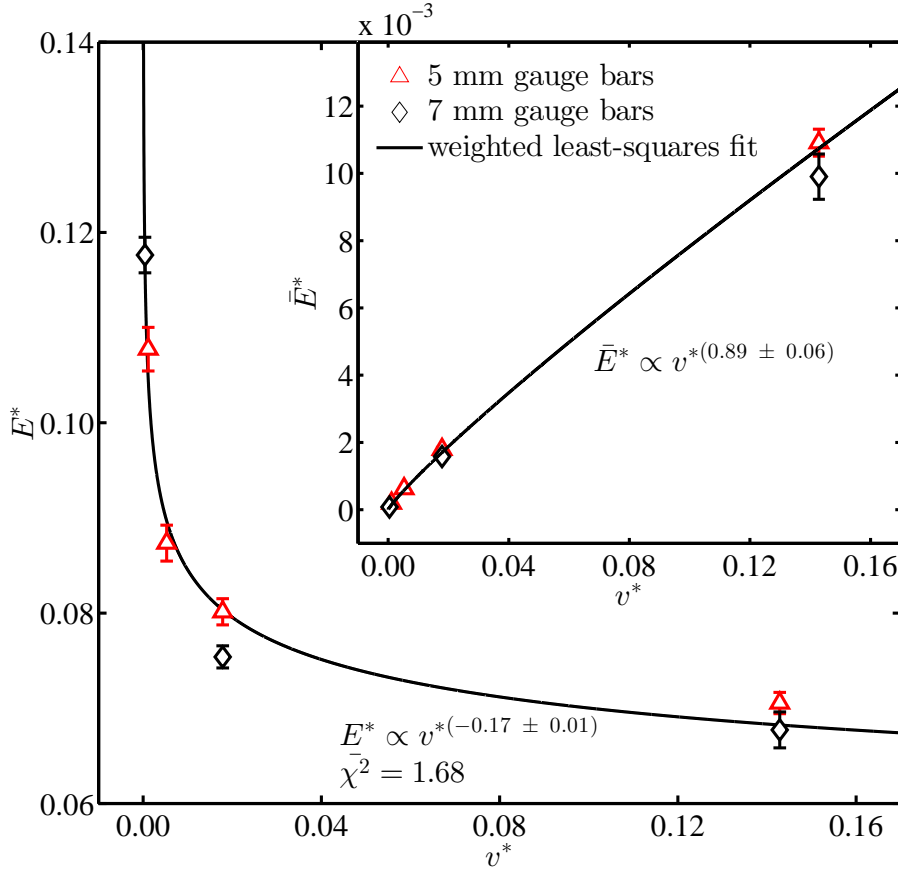


FIG. 8: The relative elastic modulus, E^* , of the 5 and 7 mm latticed test bars as a function of relative cell volume, v^* . The inset plot shows the relative elastic modulus *per unit cell*, \bar{E}^* , also as a function of v^* .

The ultimate tensile strength

The relative ultimate tensile strengths, σ_U^* , of the 5 and 7 mm latticed bars are shown in figure 9. They take values similar to those seen for E^* , that is, decreasing from $(17.7 \pm 0.2)\%$ to $(5.2 \pm 0.2)\%$ of the strengths of fully-dense test bars. Following the same approach as outlined above, three power laws, two with additional constants for l_c and σ_U^* , were trialled; they are shown as dashed, solid and dotted lines.

Once again, it is the power law of the form $\sigma_U^* = U_2 (l_c + \varepsilon_{l_c})^{n_2}$ that provides the best fit, with the unmodified power law performing significantly worse. The factors are $U_2 = 0.7 \pm 0.6$, $\varepsilon_{l_c} = 2 \pm 1$ mm and $n_2 = -1.2 \pm 0.3$. The χ^2 values for the three trialled fits are larger than obtained in the E^* analysis, reflecting statistically poorer fits overall; this is due mainly to the smaller fractional errors associated with the σ_U measurements. This has also given rise to larger uncertainties on the determined parameters U_2 , ε_{l_c} and n_2 . Interestingly, switching the dependent variable to the relative cell volume, v^* , instead of l_c , as implemented previously, did not provide an improved fit when using the unmodified power law, $\sigma_U^* \propto v^{*n}$.

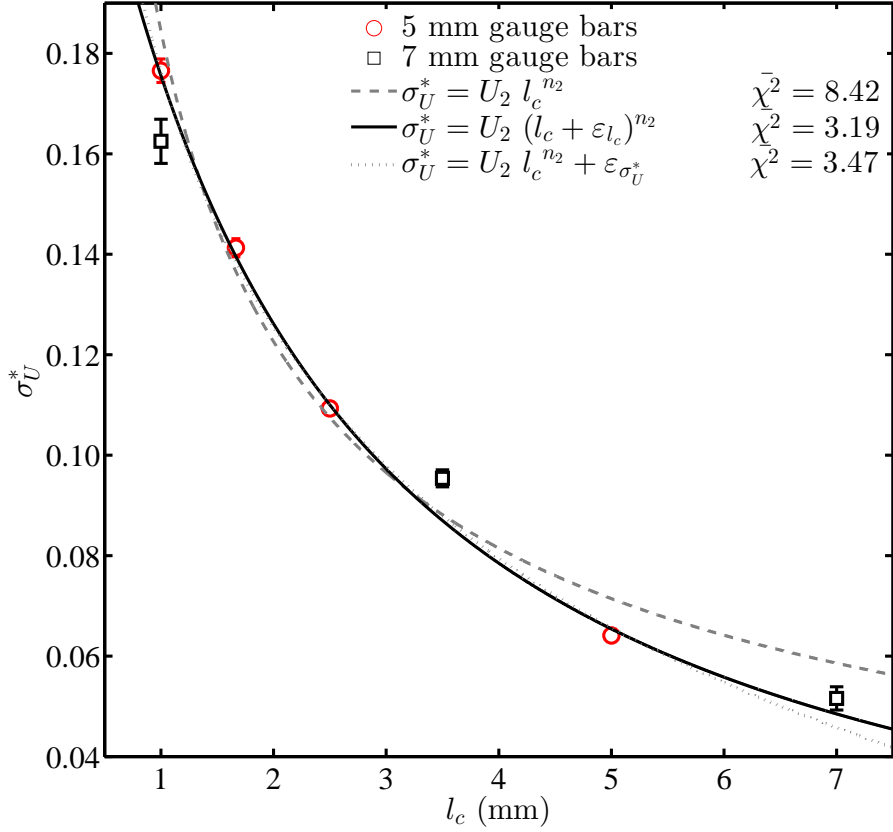


FIG. 9: The relative ultimate tensile strength, σ_U^* , of the 5 and 7 mm latticed test bars as a function of cell width, l_c . Again, a weighted least-squares power law fit, shown as a solid line, provides the dependence of σ_U^* on l_c .

The Weibull modulus

We can use the determined parameter n_2 from our best fit to estimate the Weibull modulus of our latticed parts. We speculate that the cell width dependence for σ_U^* is likely to be, or be similar to, one of those seen in equations 4 and 5. Thus, our σ_U^* values would decrease with cell size according to $l_c^{-\frac{3}{m_w}}$ or $l_c^{(\frac{1}{2}-\frac{3}{m_w})}$. The first case yields $m_w = 2.5 \pm 0.6$, whilst the second provides $m_w = 1.8 \pm 0.4$. Reasonable sources of comparison for these values are understandably scarce in the literature, owing to the lack of research on lattice structures produced by SLM. The most meaningful results currently available may be the work of Blazy *et al.* and Ramamurty *et al.*, who provide values of m_w between 8 and 16.7 ± 0.6 for some aluminium foams[24, 25], but since both the material and the manufacturing process in those works are different from our own, direct comparison is not advised. Clearly, understanding how our values of m_w relate to other work is worthy of further research.

CONCLUSIONS

The main novel finding of this investigation is that there is a dependence of the relative elastic modulus of lattice structures on the size of the cells they comprise. Our best fit suggests $E^* \propto l_c^{(-0.28 \pm 0.07)}$, though the extent to which this proportionality is applicable to lattices with different unit cell types and different global geometries is not

yet fully understood. This finding is significant because previous investigations into lattices have chiefly focussed on the influence of relative density, with any cell size effect forming part of a constant, C_1 , to be determined for each individual case. Our result could be used to develop more complete predictive models for the design of latticed parts; at its simplest it suggests a clear advantage in choosing smaller lattice unit cells if maximum stiffness is required. However, there are two important points of note; (i) a constant, which we call δ_{l_c} , was required to modify a basic power law to provide the best fit to our data, and (ii) even our modified power laws failed to properly describe the data from the test specimens with the smallest cells. The smallest cells may be outliers, or they may actually behave differently to the others.

We have shown that a possible solution to these issues lies in analysing the E^* data as a function, not of the cell width, but of the relative cell volume, v^* . This methodology provided a reasonable fit with a simpler power law than was previously achievable. An advantage of this analytical method is that it may provide a way to generalise the performance of lattices of different sizes, in much the same way that the well established use of E^* and ρ^* allows us to directly compare lattices of different materials. If this relationship proves similarly successful in further investigations, it may ultimately be found that the relative elastic modulus of lattices can be described generally by,

$$E^* = U_m \rho^{*m_1} v^{*m_2}, \quad (8)$$

where U_m is dependent only on the choice of unit cell and the global shape of the part. The implication would be that a latticed cube composed of 1000 unit cells would have the same relative elastic modulus regardless of its size, be it 20 mm wide or 100 mm wide. This requires further investigation.

Lastly, we found a cell size dependence for the ultimate tensile strength of our latticed bars; the data followed $\sigma_U^* \propto l_C^{(-1.2 \pm 0.3)}$, though, once again, the best fit was achieved only with an l_c offset, ε_{l_c} . The choice of l_c as the independent variable was appropriate for the analysis of σ_U^* data; there were no significant outliers at low cell width, and there was no improvement of fit when v^* was used instead. As above, the major implication of this finding is that smaller lattice cells should be chosen for applications where high tensile strength is required. We used our determined l_c exponent to estimate the Weibull modulus of our lattices, making the assumption that σ_U^* follows a law similar to those laid out by Gibson and Ashby for crushing strength and fracture toughness. We found $m_w = 2.5 \pm 0.6$ or $m_w = 1.8 \pm 0.4$, which are relatively small, but the lack of available sources for comparison makes a proper assessment impossible.

Acknowledgments

We would like to thank Sean Smith, Ravi Aswathanarayananaswamy, Hossein Sheykh-Poor and various teams at Renishaw Plc. for the provision of the test specimens and continued support in our collaborative projects. Thanks also to Mark East, Mark Hardy and Joe White, technicians of the Additive Manufacture and 3D Printing Research Group at Nottingham. Funding was provided by the UK Technology Strategy Board (TSB).

-
- [1] G. Chahine *et al.*, in *Solid Freeform Fabrication Symposium*, 2010.
- [2] D. Brackett *et al.*, in *Solid Freeform Fabrication Symposium*, 2011.
- [3] N. Gardan, *Int. J. Manuf. Eng.* **2014** (2014).
- [4] C. Yan *et al.*, *Mater. Design* **55**, 533 (2014).
- [5] M. Smith *et al.*, *Int. J. Mech. Sci.* **67**, 28 (2013).
- [6] K. Ushijima *et al.*, *J. Sandw. Struct. Mat.* **13**, 303 (2011).
- [7] N. A. Fleck *et al.*, *Proc. R. Soc. A* **466**, 2495 (2010).
- [8] G. W. Kooistra *et al.*, *Acta Mater.* **52**, 4229 (2004).
- [9] S. Tsopanos *et al.*, *J. Manuf. Sci. Eng. (ASME)* **132**, 041011 (2010).
- [10] Y. Shen *et al.*, *J. Sandw. Struct. Mat.* **12**, 159 (2010).
- [11] L. Gibson and M. Ashby, *Cellular Solids: Structure and properties*, Cambridge University Press, 1997.
- [12] M. Ashby, *Philos. T. Roy. Soc. A* **364**, 15 (2006).
- [13] S. P. Timoshenko and J. N. Goodier, *Theory of Elasticity*, McGraw-Hill, New York, 1970.
- [14] R. J. Roark and W. C. Young, *Formulas for stress and strain*, McGraw-Hill, London, 1976.
- [15] T. Dillard, *Caractérisation et simulation numérique du comportement Mécanique des mousses de nickel: morphologie tridimensionnelle, réponse élastoplastique et rupture*, PhD thesis, Ecole Nationale Supérieure des Mines de Paris, 2004.
- [16] D. T. Queheillalt *et al.*, *Scripta Mater.* **50**, 313 (2004).
- [17] V. S. Deshpande and N. A. Fleck, *Int. J. Solids Struct.* **38**, 6275 (2001).
- [18] C. Yan *et al.*, *J. Mater. Process Tech.* **214**, 856 (2014).
- [19] V. Deshpande *et al.*, *Acta Mater.* **49**, 1035 (2001).
- [20] R. Boyer *et al.*, editors, *Materials Properties Handbook: Titanium Alloys*, ASM International, 2007.
- [21] M. Donachie, editor, *Titanium: A Technical Guide*, ASM International, 200.
- [22] B. Vrancken *et al.*, *J. Alloy. Compd.* **541**, 177 (2012).
- [23] L. Facchini *et al.*, *Rapid Prototyping Journal* **16**, 450 (2010).
- [24] J.-S. Blazy *et al.*, *Int. J. Mech. Sci.* **46**, 217 (2004).
- [25] U. Ramamurty and A. Paul, *Acta Mater.* **52**, 869 (2004).